Thermal path integrity monitoring for IGBT power electronics modules

Mohd. Amir Eleffendi, C. Mark Johnson
University of Nottingham, Nottingham, UK

Abstract

The heat dissipation path in a power module degrades over time due to solder fatigue. Estimating level of that degradation requires accurate measurements of junction temperature in real-time. Temperature sensitive electrical parameters (TSEPs) and model estimates are two techniques to estimate junction temperature but they suffer from large inaccuracies and uncertainties during measurement and model identification process. This paper presents a non-invasive technique which incorporates model estimates with real-time measurements of $V_{CE(ON)}$ to accurately track junction temperature of an IGBT and to monitor the health state of the thermal path in a power module. The technique is built upon the algorithm of Kalman filter which gives optimal estimates of system states in the presence of inaccurate and corrupted measurements. The adaptive property of Kalman filter allows consistent estimate of junction temperature under time-varying conditions of the thermal path due to solder fatigue.

1 Introduction

Power electronics industrial requirements have increased significantly in recent years towards higher integration and functionality. That led to higher power density and limited heat dissipation capabilities due to smaller sizes and higher power ratings, the matter that puts an overhead to reliability issues of power electronics modules. They are used in utility power systems, power conversion, traction, aerospace and industrial drive circuits. They operate in harsh environments which makes them one of the most common components and the most prone to failures in power systems [1]. Therefore, high reliability standards are considered during the design phase to increase lifetime of power modules. Yet, monitoring health state during real-time operation is highly desirable to minimize periodic maintenance and systems down-time by conducting preventive and predictive maintenance which consequently increases lifetime, maintainability and safety of power systems.

Temperature is one of the key parameters that drive degradation processes in power electronics modules. Thermo-mechanical stresses are generated in the contacting surfaces of the multilayer structure due to the mismatch in coefficients of thermal expansion (CTEs) of materials constituting the structure. Over time, voids and cracking start to initiate and propagate throughout different sites in the structure which constitutes the heat conduction path in the power module. Those cracks, voids and delamination increase thermal resistance of heat conduction path which in turn increases device temperature [2].

Two sites most vulnerable for cracking are solder joint layer (between substrate and baseplate) and die-attach layer. Cracks are initiated at the edges of the layer and propagate towards the center [2]. The increment of device temperature may lead to other failures such as latch-up and burn-out failures due to chip overheating, and may accelerate other failure mechanisms such as wire-bond lift-offs [2,3]. Therefore, monitoring health state of heat conduction path during normal field operation is essential for in-field reliability of power modules.

The key idea of condition monitoring in general is based on real-time measurements of failure indicators, and in the case of power electronics module junction temperature is the key indicator of thermal path degradation. But unfortunately this measurement cannot be done by direct methods due to inaccessibility to the measurement point. Therefore indirect methods are used to estimate junction temperature. Some of these methods are based on model estimates [4] which cannot track the real temperature profile as cracks propagate in the structure and alter the thermal path. On the other hand, temperature sensitive electrical parameters (TSEPs) can be used to get information about junction temperature. But real-time measurement of these parameters is difficult because of high currents and voltages which reduce measurement accuracy of parameter such as $V_{CE(ON)}$ [5, 6], while fast switching characteristics of power devices require high time resolution to capture switching parameters such as dv/dt, t_{don} and t_{off} [7], in addition to the relatively low sensitivity of temperature sensitive electrical parameters (TSEPs) to junction temperature [7, 8] and the wide-band noise and interference from the surrounding environment. Not to forget the contribution of loading conditions and gate drive characteristics on the measured variables and the effect of switching signal which corrupt the continuity of the measurements. That makes the process of resolving junction temperature information from measurements of temperature sensitive electrical parameters (TSEPs) a very challenging task. In consequence, it is imperative to combine real-time measurements of TSEPs and model estimates to employ all available knowledge to resolve junction temperature and health state of the thermal path.

Only few methods were proposed in literature to monitor the health state of heat conduction path during normal operation of power modules. Dawei et al [9] proposed a method to estimate the change in thermal resistance due to solder fatigue by employing measurements of case temperature, power-loss model and a thermal model. Anderson et al [10] proposed a data-based method utilizing measurements of current and voltage to estimate on-resistance of the device and employs PCA algorithm to extract features of degradation from measured signals. Dawei et al [11] introduced a method based on the output harmonics of an inverter as an indicator of solder fatigue. Musallam [12] used a real-time thermal model with an infrared camera to monitor thermal path degradation and to assess the change in thermal resistance due to solder fatigue.

This paper studies through simulation a monitoring approach based on the algorithm of Kalman filter to estimate junction temperature under degradation condition of power module thermal path. The method combines a model estimate of T_J with a real-time measurement of $V_{CE(ON)}$ as a temperature sensitive electrical parameters. Junction to ambient thermal resistance $R_{\theta Ja}$ is used to characterize the degradation in the thermal path. Next section describes thermal model formulation and Kalman filter algorithm. Section 3 describes experimental identification of baseline and degraded thermal model. Section 4 presents simulation results and the conclusion is presented in section 5.

2 Problem Formulation

2.1 Derivation of the thermal model

The heat conduction path of a power module can be described by an equivalent electrical circuit of Foster network with an infinite number of RC elements as is shown in Figure 1. The thermal impedance of the heat conduction path describes the response of a thermal system to a step power input. It is described by the ratio of the difference between junction temperature and a reference temperature to the input power:

$$Z_{\theta ja}(t) = \frac{T_j(t) - T_a}{P_d} \tag{1}$$

where T_j is the junction temperature, Ta is the ambient temperature and P_d is the power dissipation. Foster network model shown in Figure 1 is a behavioural model of the thermal system, that is RC elements of the model have no physical meaning. They have no relation to the real thermal resistances and thermal capacitances of any layer of the structure with the exception of the total sum of thermal resistances which equals the total thermal resistance of the structure. Each RC element has a time constant τ=RC and captures one zero-pole pair of the thermal system. The transfer function of foster network can be represented by:

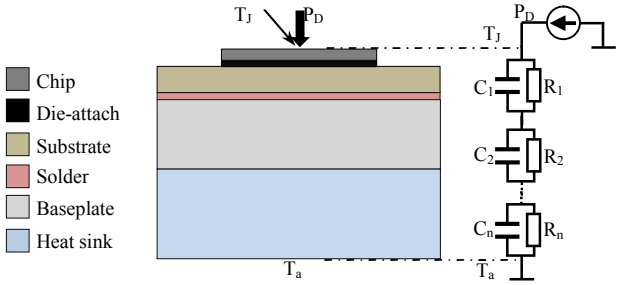

Figure 1 the multilayer structure of a power module and its equivalent foster network

$$Z_{\theta ja}(s) = \frac{b_{n-1}s^{n-1} + b_{n-2}s^{n-2} + \cdots + b_0}{a_n s^n + a_{n-1}s^{n-1} + \cdots + a_1 s + 1} \tag{2}$$

where a and b are coefficients of the transfer function and can be identified by least squares fitting and s is the complex variable. In order for this transfer function to represent a proper impedance function of a foster network it should satisfy a set of conditions [13]: 1) poles and zeros lay on the real negative axis. 2) Poles and zeros must alternate on that axis. 3) The nearest singularity to the origin must be a pole and the nearest singularity to infinity must be a zero. 4) The residues should be real positive. Those conditions should be satisfied by the curve fitting algorithm during the identification process in order to generate a proper set of RC parameters.

The partial fraction expansion form highlights the decoupled nature of the foster network and simplifies numerical solution of the system [14]:

$$Z_{\theta ja}(s) = \sum_{i=1}^{n} \frac{k_i}{s + p_i} \tag{3}$$

where n is the model order or the number of RC elements, k_i and p_i are residues and poles of the transfer function respectively. After a and b coefficients in (2) are identified and the transfer function is expanded into form (3) the values of RC elements can be calculated from the poles p_i and the residues k_i by the following formulas:

$$R_i = \frac{k_i}{|p_i|}, \quad C_i = \frac{1}{|p_i|} \tag{4}$$

Deriving a state-space representation of the model is necessary for the derivation of Kalman filter which is discussed in the following section. Hence, the partial-fraction form in (3) is transferred into a state-space representation by considering the parallel form of a state-space model. This form is derived directly from a partial fraction expansion and leads to a diagonal system matrix where system poles p_i are elements of the main diagonal, while residues k_i are elements of the input matrix. This matrix is extended with a second column to account for the ambient temperature as a second input to the system. The ambient temperature is assumed to be additive to the output therefore the second column is a zero column. The resulting state-space representation of the thermal model is:

$$\dot{x}(t) = Ax(t) + Bu(t) \qquad (state\ equation)$$
$$T_J(t) = Cx(t) + Du(\mathrm{t}) \qquad (output\ equation)$$

$$A = \begin{bmatrix} p_1 & 0 & 0 & \cdots & 0 \\ 0 & p_2 & 0 & \cdots & 0 \\ 0 & 0 & p_3 & \ldots & 0 \\ \vdots & \vdots & \vdots & \ddots & \vdots \\ 0 & 0 & 0 & \ldots & p_n \end{bmatrix} \quad B = \begin{bmatrix} k_1 & 0 \\ k_2 & 0 \\ k_3 & 0 \\ \vdots & \vdots \\ k_n & 0 \end{bmatrix} \qquad (5)$$

$$C = [1 \quad 1 \quad 1 \quad \ldots \quad 1] \qquad D = [0 \quad 1]$$

where system states vector $\boldsymbol{x}$ represents the differential temperatures across each RC element of the network, $\boldsymbol{u=[P_d,\ T_a]}$ is the system input vector where $\boldsymbol{P_d}$ is the power dissipation and $\boldsymbol{T_a}$ is the ambient temperature. The output equation represents junction temperature $\boldsymbol{T_J}$ which is the total sum of system states. $\boldsymbol{A_{n\times n}}$ is the system matrix, $\boldsymbol{B_{n\times 2}}$ is the input matrix, $\boldsymbol{C_{1\times n}}$ is the output matrix and $\boldsymbol{D_{1\times 2}}$ is the feed-forward matrix.

2.2 Time-Varying Kalman Filter

A Kalman filter estimates the states of a linear system assuming an input vector is known and at least one measurement vector is available as feedback from the real system. In our case, the model is the thermal model described in (5) which represents *apriori* knowledge, the inputs are P_D and T_a which are known and the measurement of T_J is provided by an estimate from $V_{CE(ON)}$ measurement as *aposteriori* knowledge. It is assumed that the model dynamics and the measurements are disturbed by an uncorrelated white Gaussian noise and that the noise covariance is known. Process noise accounts for uncertainty in the modeling process, while measurement noise accounts for sensor noise and interferences superimposed on $V_{CE(ON)}$. The model in (5) is discretized with a time step T_s using Euler backward method and is modified with process and measurement noise terms so that the discretized model becomes:

$$x[k+1] = Fx[k] + Gu[k] + Hw[k]$$
$$T_j[k] = Cx[k] + Du[k] + v[k] \qquad (6)$$

where $\mathbf{w_{n\times 1}}$ is the process noise, $\mathbf{v_{1\times 1}}$ is the measurement noise, $\mathbf{F_{n\times n}}$ is the state transition matrix, $\mathbf{G_{n\times 2}}$ is the input matrix, $\mathbf{H_{n\times n}}$ is the process noise gain matrix.

Kalman filter works in two steps, first a priori estimate of states $\hat{\boldsymbol{x}}\boldsymbol{[k+1|k]}$ is calculated given a past estimate $\hat{\boldsymbol{x}}\boldsymbol{[k|k]}$ and the current input vector $\boldsymbol{u[k|k]}$ in a prediction step. Then a correction step is carried out using a measurement $\boldsymbol{T_J[k]}$ where an error signal $\boldsymbol{e[k]}$ is generated as the difference between the measurement $\boldsymbol{T_J[k]}$ and the estimate $\hat{\boldsymbol{T}}_{\boldsymbol{J}}\boldsymbol{[k]}$. This error is fed-back through Kalman gain matrix $\boldsymbol{K[k]}$ to calculate a posteriori estimate $\hat{\boldsymbol{x}}\boldsymbol{[k|k]}$. The algorithm updates $\boldsymbol{K[k]}$ in every iteration to minimize the mean value of the error signal $\boldsymbol{e[k]}$. This adaptive property allows the algorithm to track junction temperature under time-varying conditions such as degradation of the heat conduction path. Kalman filter is implemented by iterating through the following set of equations:

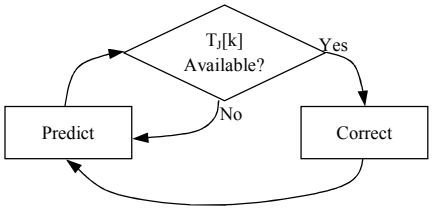

Figure 2 the sequence of Kalman filter steps

$$\textit{Predict}\begin{cases} \hat{x}[k+1|k] = F\hat{x}[k|k] + Bu[k|k] \\ P[k+1|k] = FP[k|k]F^T + HQ_kH \end{cases}$$
$$\textit{Correct}\begin{cases} K[k] = P[k+1|k]C[CP[k+1|k]C^T + R_k]^{-1} \\ \hat{x}[k|k] = \hat{x}[k+1|k] + K[k]e[k] \\ P[k|k] = [I - K[k]C]P[k+1|k] \end{cases} \qquad (7)$$

where $\boldsymbol{P[k+1|k]}$ is the priori estimate of error covariance and $\boldsymbol{P[k|k]}$ the posteriori estimate, $\boldsymbol{Q}$ is the process noise covariance, $\boldsymbol{R}$ is the measurement noise covariance and $\boldsymbol{I}$ is the identity matrix. Matrices $\boldsymbol{Q}$ and $\boldsymbol{R}$ are determined as tuning parameters to get the best performance of the filter [15].

The problem of missing data is accounted for by running the filter in the prediction step only when measurement of $\boldsymbol{T_J[k]}$ is unavailable. In this case $\hat{\boldsymbol{T}}_{\boldsymbol{J}}\boldsymbol{[k]}$ is calculated only from $\boldsymbol{u=[P_D,\ T_a]}$ and the history of temperature profile. Whenever a new measurement of $\boldsymbol{T_J[k]}$ is available the correction step is carried out. This flow of implementation is described in Figure 2 and is controlled by manipulating the measurement matrix $\boldsymbol{C}$ according to $\boldsymbol{T_J[k]}$ availability such that when $\boldsymbol{T_J[k]}$ is missing $\boldsymbol{C}$ is made to be $\boldsymbol{C=0}$ which forces the posteriori estimate to be equal to the priori estimate $\hat{\boldsymbol{x}}\boldsymbol{[k|k]=}\hat{\boldsymbol{x}}\boldsymbol{[k+1|k]}$ and similarly the posteriori error covariance to be equal to the priori one $\boldsymbol{P[k|k]=P[k+1|k]}$.

3 Thermal and Electrical Model Identification

3.1 Identification of Baseline and Degraded Thermal models

The process of initiating failures in the thermal path through thermal or power cycling tests are a time consuming process and it is difficult to control the dominant failure mechanism taking place in the cycled samples. Therefore, an emulation of a degraded thermal path is conducted by inserting thermal pads in between the substrate and the baseplate of an IGBT module test sample. Thermal pads used are aluminium nitride AlN with a thickness of 1mm. Thermal pad 1 has a solid design while thermal pad 2 has a punched design so that thermal resistance of Pad 2 is higher that Pad 1. A holder is designed to clamp the substrate on top of the thermal pad and the baseplate using clamps at the edges of the substrate. The baseplate is then fixed to a cold plate which is connected to a water cooling system that controls water temperature to be 19°C.

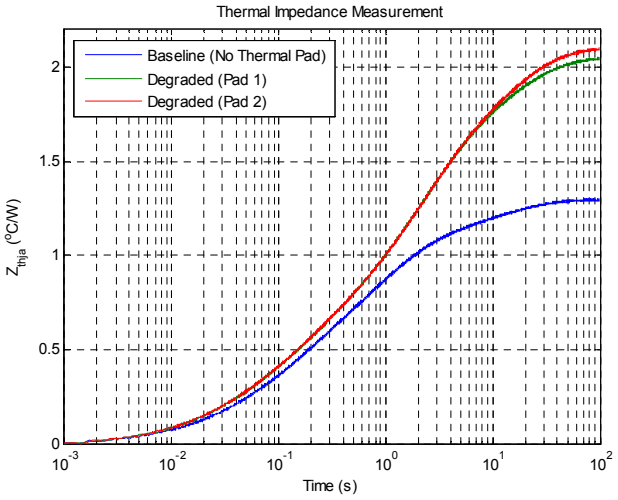

Figure 3 Experimental thermal impedance measurements of Baseline and Degraded IGBT module

Table 1 The identified parameters of the thermal model

	Foster network parameters							
	R1	***R2***	***R3***	***R4***	***C1***	***C2***	***C3***	***C4***
Baseline	0.147	0.384	0.522	0.225	0.192	0.450	2.087	51.813
Pad 1	0.241	0.417	0.828	0.529	0.146	0.600	2.576	28.089
Pad 2	0.244	0.416	0.814	0.594	0.146	0.589	2.635	25.252

Junction to ambient thermal impedance $Z_{\theta ja}$ is determined by measuring the cooling curve of the junction temperature of the IGBT using a thermal impedance analyser. The chip is self-heated by passing a current of 25A which generates a power dissipation of 49W. The thermal system arrived to thermal equilibrium after 100s. The current is then bypassed and 40mA current is injected into the IGBT to allow measuring V_{CE} which is sampled with a frequency of 10kHz.

This process is repeated 100 times and V_{CE} measurement is averaged to reduce measurement noise. The data is then resampled by a logarithmic time vector to emphasize the behaviour of faster poles and to reduce data size. A calibrated model $T_J=f(V_{CE})$ is then used to get the junction temperature profile which is shifted and mirrored to generate the heating curve.

The thermal impedance is measured for three cases: 1) baseline case where no thermal pad is used 2) with thermal pad 1 which increased thermal resistance by 58% 3) with thermal pad 2 which increased thermal resistance by 62%. Figure 3 shows measurements of thermal impedance for all three cases.

Parameter identification process is carried out by least squares algorithm to fit the model of (2) to data shown in Figure 3. Model order is determined by examining convergence of the fitting residual with increased model order. It is found that the residual converged to a constant value after a model order of 4. Therefore the model is chosen to be of 4th order. RC values of the three models by least-squares fitting are presented in Table 1.

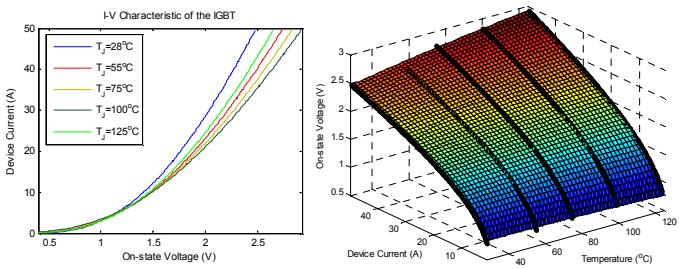

(a) (b)

Figure 4 (a) the I-V characteristic of an IGBT device **(b)** the electrical model of an IGBT device

3.2 Identification of Electrical Model

The electrical model of the IGBT chip is obtained from the I-V characteristic. A curve tracer is used to obtain I-V curves at multiple junction temperatures. The test module was fixed on a hot plate and the temperature is measured using a thermocouple at the top surface of the chip. All curves are obtained at a gate voltage of 15V. I-V curves as a function of temperature are shown in Figure 4. Using least squares algorithm a polynomial of 2nd order to temperature and 4th order to current is found to give a good fit to data with R^2=0.9995. The modeling error bounds are ±0.02V. The electrical model is shown in Figure 4 and is described by the following polynomial:

$$\begin{aligned} V(T,I) = {} & a_{00} + a_{10}*T + a_{01}*I + a_{20}*T^2 \\ & + a_{11}*T*I + a_{02}*I^2 + a_{21}*T^2*I \\ & + a_{12}*T*I^2 + a_{03}*I^3 + a_{22}*T^2*I^2 \\ & + a_{13}*T*I^3 + a_{04}*I^4 \end{aligned} \quad (8)$$

4 Simulation and Results

A Matlab/Simulink model is used to test the algorithm of Kalman filtering for purpose of junction temperature estimate and thermal path monitoring. The model shown in Figure 5 simulates the electro-thermal behaviour of an IGBT device in a Voltage-Source Inverter (VSI). The feedback of T_J into the electrical model allows thermal degradation to affect electrical parameters i.e. power dissipation P_D and $V_{CE(ON)}$. The switching PWM signal is generated with a switching frequency of 1kHz for a sinusoid modulation signal with a 50A amplitude and a frequency of 8Hz. Only conduction power loss is considered in the simulation and is calculated as function $P_D=f(I_C,V_{CE(ON)},T_j,\rho,F_s)$ of duty cycle ratio ρ, switching

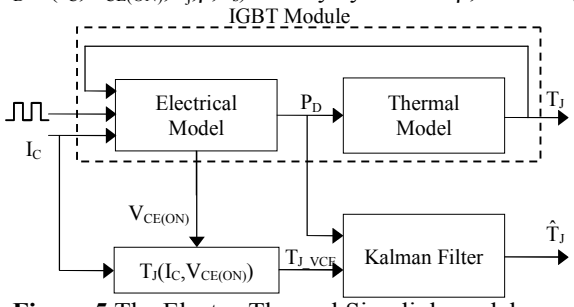

Figure 5 The Electro-Thermal Simulink model

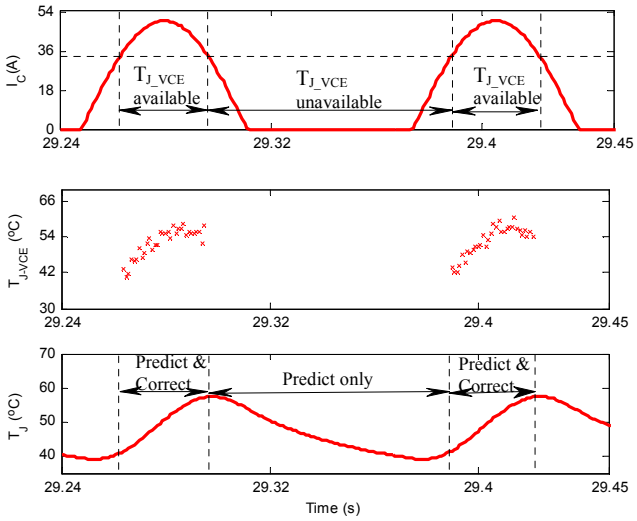

Figure 6 availability of the estimate T_{J_VCE} and the corresponding steps of Kalman filter

frequency F_s, junction temperature T_j, device current I_C and on-state voltage $V_{CE(ON)}$. The outputs of the electrical model are the power dissipation P_D and $V_{CE(ON)}$. An additive white Gaussian noise is superimposed on $V_{CE(ON)}$ to simulate measurement noise in a real inverter. P_D is fed to the thermal model and to Kalman Filter as the input signal u[k], and $V_{CE(ON)}$ is used to produce an estimate of junction temperature T_{J_VCE} which is passed to Kalman filter as the measurement signal T_J[k]. The estimate T_{J_VCE} is produced by a model $T_{J\_VCE}(I_C,V_{CE(ON)})$. This model although is obtained from the same I-V curves in Figure 4 unlike (8) is more critical because of the measurement noise presented in $V_{CE(ON)}$. This noise leads to large errors in the estimate of T_J at low I_C due to lower sensitivity of $V_{CE(ON)}$ to T_J at low currents. For example, assume $V_{CE(ON)}$ measurement error is ±20mV that contributes to an error ±22°C in T_{J_VCE} when I_C=10A where sensitivity is about 0.92mV/°C while the same error contributes to ±5°C when I_C=45A where sensitivity is about 4mV/°C. Hence, to avoid large estimation errors in T_{J_VCE} signal the model $T_{J\_VCE}(I_C,V_{CE(ON)})$ is fit to the data where I_C>35A.

Consequently, availability of the estimate T_{J_VCE} is limited to when I_C>35A during half period of the phase current. That limits the implementation of the correction step which uses T_{J_VCE} estimate to the time when I_C>35A as explained in Figure 6 while the filter estimates junction temperature T_J utilizing only the thermal model in a prediction step for the rest of the current period. The result of simulation is shown in Figure 7 which depicts the operation of the Kalman filter. The corrupted measurement of the junction temperature T_{J_VCE} obtained from $V_{CE(ON)}$ is

Table 2 Effects of $V_{CE(ON)}$ measurements on Estimation Error

	Estimation Error							
	MAE				σ^2			
Q. (mV)	**100**	**50**	**19.5**	**1.22**	**100**	**50**	**19.5**	**1.22**
Samples Num. = 8	2.40	2.17	1.66	1.61	10.65	5.69	4.84	4.24
Samples Num.= 16	1.88	1.70	1.40	1.37	8.03	4.35	3.37	3.14
Samples Num.= 32	1.35	1.23	1.17	1.15	6.58	3.48	2.65	2.64

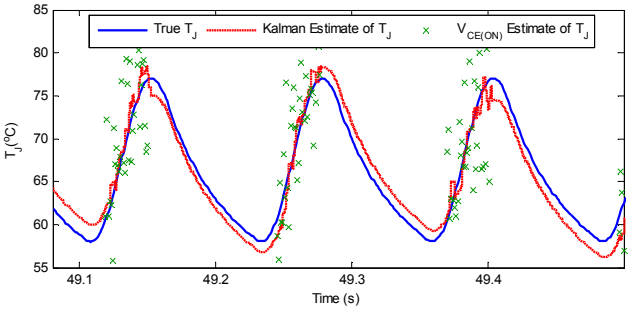

Figure 7 Kalman Estimate of T_J compared to True T_J and $V_{CE(ON)}$ estimate T_{J_VCE}

used by the filter to correct model estimates $\hat{T}_J$ by minimizing the mean of the error signal between T_{J_VCE} and $\hat{T}_J$.

This error signal is critical for the performance of the algorithm. And since it is generated from the estimate T_{J_VCE} it is important to examine the effect of $V_{CE(ON)}$ measurement accuracy and sampling rate on the performance of the algorithm. Measurement accuracy and sampling rate are represented by quantization error (Q) and samples number respectively. Table 2 shows the mean absolute error (MAE) and the variance of the error signal for different Q and samples number. It is obvious that estimation accuracy can be improved by increasing measurement accuracy and sampling rate which could be limited for practical reasons. Still, fair estimates can be achieved with lower accuracy and lower sampling rate.

Thermal path degradation is simulated by changing thermal model's parameters from baseline to degraded cases as identified in Table 1 while other parts of the model are fixed. Simulation results are presented in Figure 8 where the true T_J of the baseline and degraded thermal path are shown in Figure 8(a) and the corresponding estimates $\hat{T}_J$ are shown in Figure 8(b). It can be seen that Kalman estimate is consistent for large changes as well as small deviations in the model parameters. That explains robustness of the Kalman filter towards modeling uncertainties and time-varying models which allows using its estimate to monitor the state of the thermal path in IGBT modules.

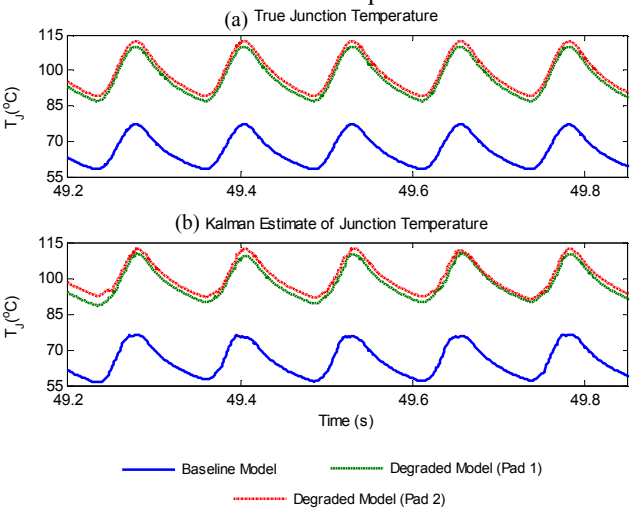

Figure 8 (a) True junction temperatue **(b)** Kalman Estimate of junction temperature

Table 3 Measured and Estimated Thermal resistance

Mean Value / System State	T_m (^{O}C)	$\hat{T}_m$(^{O}C)	P_m (W)	Measured $R_{\theta ja}$ (^{O}C/W)	Estimated $R_{\theta ja}$ (^{O}C/W)
Baseline	66.32	65.78	38.25	1.29	1.27
Degraded (Pad 1)	97.01	98.75	39.70	2.04	2.06
Degraded (Pad 2)	99.10	100.23	39.77	2.1	2.09

In order to assess the level of degradation in the thermal path the junction-to-ambient thermal resistance $R_{\theta ja}$ is calculated using Kalman estimate $\hat{T}_J$ under constant operational conditions where a time window of 5s is used to calculate the mean of junction temperature estimate $\hat{T}_J$ and the mean of power dissipation P_D. Then $R_{\theta ja}$ is estimated using the following relationship:

$$R_{\theta ja} = \frac{\hat{T}_m - T_a}{P_m} \quad (9)$$

where $\hat{T}_m$ is the mean value of Kalman estimate $\hat{T}_J$, P_m is the mean value of power dissipation and T_a is the ambient temperature. Table 3 shows the estimated junction-to-ambient thermal resistance for healthy and degraded cases calculated using Kalman estimate $\hat{T}_J$ and compared to the experimentally measured thermal resistance using the thermal impedance curve in Figure 3. It is shown that the mean value of junction temperature is increasing as well as power dissipation in the chip due to thermal path degradation. That increment of junction temperature is a result of higher thermal resistance. The estimated junction-to-ambient thermal resistance $R_{\theta ja}$ matches with the measured $R_{\theta ja}$ which describes the adaptive property of Kalman filter estimate of junction temperature for purposes of thermal path monitoring.

5 Conclusion and Future Work

This paper introduced an approach to accurately estimate junction temperature of an IGBT power module in real-time. It is based on Kalman filter algorithm which incorporates *apriori* model estimate with inaccurate and corrupted *aposteriori* knowledge from real-time measurements of temperature sensitive electrical parameters (TSEPs). This work used $V_{CE(ON)}$ as a temperature sensitive electrical parameter to get information about junction temperature. The temperature estimate given by $V_{CE(ON)}$ is noisy and intermittent due to the nonlinearity of the I-V characteristic of an IGBT, low temperature sensitivity and the variable phase current in an inverter. It has been shown that this corrupted information of junction temperature produced by $V_{CE(ON)}$ can be incorporated with a model estimate through the use of Kalman filter to accurately estimate junction temperature and allows real-time condition monitoring of the thermal path of a power module. The stochastic formulation of the thermal model used by Kalman filter takes into account modeling uncertainties while the adaptive nature of Kalman gain matrix keeps estimate updated to the time-varying conditions of the thermal path. Consequently, allows consistent estimate of junction temperature as solder fatigue develops and cracks propagate through the multilayer structure of the power module. The effect of $V_{CE(ON)}$ measurement inaccuracies and sampling rate was studied through simulation and results have shown that the estimate error can be reduced by reducing quantization error of the measurement circuit and increasing sampling rate of $V_{CE(ON)}$ during a current period.

The potential use of Kalman filter in the field of power electronics has been studied through simulation. It shows robustness and consistency in estimating the junction temperature of an IGBT. It allows developing an efficient real-time condition monitoring for power modules regardless of application and system topology if it is implemented on gate drives to monitor individual modules. Experimental setup is being prepared for validating the algorithm.

6 References

[1] Y. Shaoyong, A. Bryant, P. Mawby, X. Dawei, R. Li, P. Tavner, An Industry-Based Survey of Reliability in Power Electronic Converters, Industry Applications, IEEE Transactions on, 47 (2011) 1441-1451.

[2] M. Ciappa, Selected failure mechanisms of modern power modules, Microelectronics Reliability, 42 (2002) 653-667.

[3] V.A. Sankaran, C. Chen, C.S. Avant, X. Xu, Power cycling reliability of IGBT power modules, Industry Applications Conference, 1997. Thirty-Second IAS Annual Meeting, IAS '97., Conference Record of the 1997 IEEE1997, pp. 1222-1227 vol.1222.

[4] M. Musallam, C.M. Johnson, Real-Time Compact Thermal Models for Health Management of Power Electronics, Power Electronics, IEEE Transactions on, 25 (2010) 1416-1425.

[5] K. Yong-Seok, S. Seung-Ki, On-line estimation of IGBT junction temperature using on-state voltage drop, Industry Applications Conference, 1998. Thirty-Third IAS Annual Meeting. The 1998 IEEE1998, pp. 853-859 vol.852.

[6] D. Wagenitz, A. Hambrecht, S. Dieckerhoff, Lifetime Evaluation of IGBT Power Modules Applying a Nonlinear Saturation Voltage Observer, Integrated Power Electronics Systems (CIPS), 2012 7th International Conference on2012, pp. 1-5.

[7] H. Kuhn, A. Mertens, On-line junction temperature measurement of IGBTs based on temperature sensitive electrical parameters, Power Electronics and Applications, 2009. EPE '09. 13th European Conference on2009, pp. 1-10.

[8] Y. Avenas, L. Dupont, Z. Khatir, Temperature Measurement of Power Semiconductor Devices by Thermo-Sensitive Electrical Parameters—A Review, Power Electronics, IEEE Transactions on, 27 (2012) 3081-3092.

[9] X. Dawei, R. Li, P. Tavner, Y. Shaoyong, A. Bryant, P. Mawby, Monitoring solder fatigue in a power module using the rise of case-above-ambient tem-

perature, Energy Conversion Congress and Exposition (ECCE), 2010 IEEE2010, pp. 955-962.

[10] J.M. Anderson, R.W. Cox, On-line condition monitoring for MOSFET and IGBT switches in digitally controlled drives, Energy Conversion Congress and Exposition (ECCE), 2011 IEEE2011, pp. 3920-3927.

[11] X. Dawei, L. Ran, P. Tavner, Y. Shaoyong, A. Bryant, P. Mawby, Condition Monitoring Power Module Solder Fatigue Using Inverter Harmonic Identification, Power Electronics, IEEE Transactions on, 27 (2012) 235-247.

[12] M. Musallam, C.M. Johnson, Monitoring through-life thermal path degradation using real time thermal models, Power Electronics Specialists Conference, 2008. PESC 2008. IEEE2008, pp. 738-743.

[13] F.F. Kuo, Network analysis and synthesis, John Wiley & Sons Australia, Limited 1966.

[14] N.S. Nise, Control Systems Engineering, John Wiley & Sons, Incorporated 2011.

[15] M.S. Grewal, A.P. Andrews, Kalman Filtering: Theory and Practice Using MATLAB, Wiley 2011.